Acta Oncologica Vol. 35, No. 7, pp. 849–856, 1996

MODELLING OF AUGER-INDUCED DNA DAMAGE BY INCORPORATED ^{125}I

HOOSHANG NIKJOO, ROGER F. MARTIN, DAVID E. CHARLTON, MICHEL TERRISSOL, SIVAMANY KANDAIYA and PAVEL LOBACHEVSKY

We have analyzed a newly available high resolution and precision repeat of the original Martin and Haseltine experiment which includes the influence of DMSO on the results. The new model includes the production and diffusion of radical species and ·OH radical attack on DNA as well as the direct hits. Calculations of single-strand breaks use individual Auger electron along with the tracks of electrons and radical species superimposed on an atomistic model of B-DNA. Comparison of the preliminary calculations with the experiment supports the earlier choice of data for the amount of energy required to produce a single-strand break, i.e. 17.5 eV. In a separate simulation we found that an average of less than two ionizations inducing a single-strand break gave the best fit to experimental data. Direct hits were found to be predominantly occurring at short range while the damage by ·OH radicals was mainly of the long-range type.

Early experimental observations of the effects of ^{125}I incorporated into the DNA indicated that each decay produces about one double-strand break (dsb) (1). At that time it was not possible to examine in more detail the nature of the break. Later, in one of the earliest applications of molecular biology techniques to radiation biology, Martin and Haseltine (2), showed that the single-strand breaks thought to be responsible for the double-strand break could be distributed over several base pairs and so it was likely that the dsb was not a simple scission of the DNA. They measured the distribution of the greatest distances of single-strand breaks from the base carrying the ^{125}I in the strand containing the decay. Most single-strand breaks were produced within 5 base pairs of the decay.

Received 20 September 1995.
Accepted 11 June 1996.
From the MRC Radiation and Genome Stability Unit, Chilton, Didcot, UK (H. Nikjoo), Peter MacCallum Cancer Institute, Melbourne, Australia (R. F. Martin, S. Kandaiya, P. Lobachersky), Concordia University, Montreal, Quebec, Canada (D. E. Charlton) and CPAT, Paul Sabatier University, Toulouse, Cedex, France (M. Terrissol).
Correspondence to: Dr H. Nikjoo, MRC Radiation and Genome Stability Unit, Harwell, Oxfordshire OX11 0RD, UK, tel: +44 1235 820 666 ext 203, fax: +44 1235 834 776, e-mail: hn@baha.har-rbu.mrc.ac.uk
Paper presented at the Third International Symposium on Biophysical Aspects of Uuger Processes, August 24–25, Lund, Sweden.

In theoretical studies a Monte Carlo treatment of the ^{125}I decay produced sets of electron spectra for individual decays and the development computer codes to simulate the deposition of energy along individual electron tracks (3, 4). An average spectrum is shown in Fig. 1, generated by the code 'I125cascade', with an average number of 20.9 electrons and 19.4 keV average total electron energy per decay. Charlton (5) combined these two techniques to calculate the energy deposited in double stranded DNA in sequential base pairs (bp) from the site of the decay for DNA wrapped around the nucleosome. Results of this calculation were that in the DNA strand containing the decaying iodine atom there is a very rapid decrease in the average energy deposited away from the location of the decay. The mean energy deposited decreased by a factor of 50 at 10 bp from decay site. It was also shown that the directly deposited energy on double stranded DNA varied considerably from decay to decay.

The rapid decrease of energy deposited with distance from the decay was remarkably similar to the decrease in single strand breaks observed by Martin & Haseltine (2) and an attempt was made to model this experiment (6, 7). Here a model of the DNA was constructed, Fig. 2a, reducing the complex molecular structure to simple volumes representing the bases (assumed not to participate in strand breakage) and the sugar-phosphates moieties of the two strands where energy deposition could cause strand

 ISSN 0284-186X

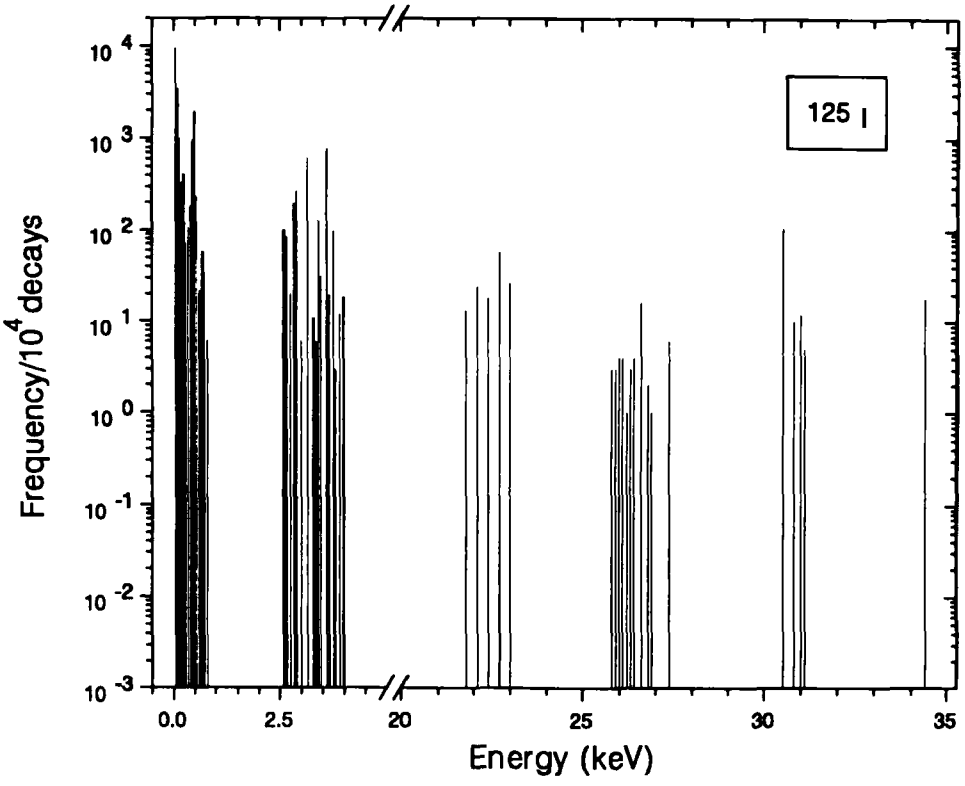

Fig. 1. Frequency distribution energies released in ^{125}I decay. Data are presented for 10^4 decays. The average number of electrons per decay is 20.1 and the average electron energy per decay is 19.8 keV. Note that the region on the energy scale not containing any electrons in the spectrum is not shown.

breaks. Energy depositions in sugar-phosphate skeleton of the DNA were calculated for the strand containing the decay and breaks were assigned according to the energy deposited in the sugar-phosphate volumes. It was found that 17.5 eV of energy deposited on average in the sugar-phosphate volume produced reasonable agreement with the experimental results of Martin and Haseltine. The figure of 17.5 eV which is the lower threshold for produc-

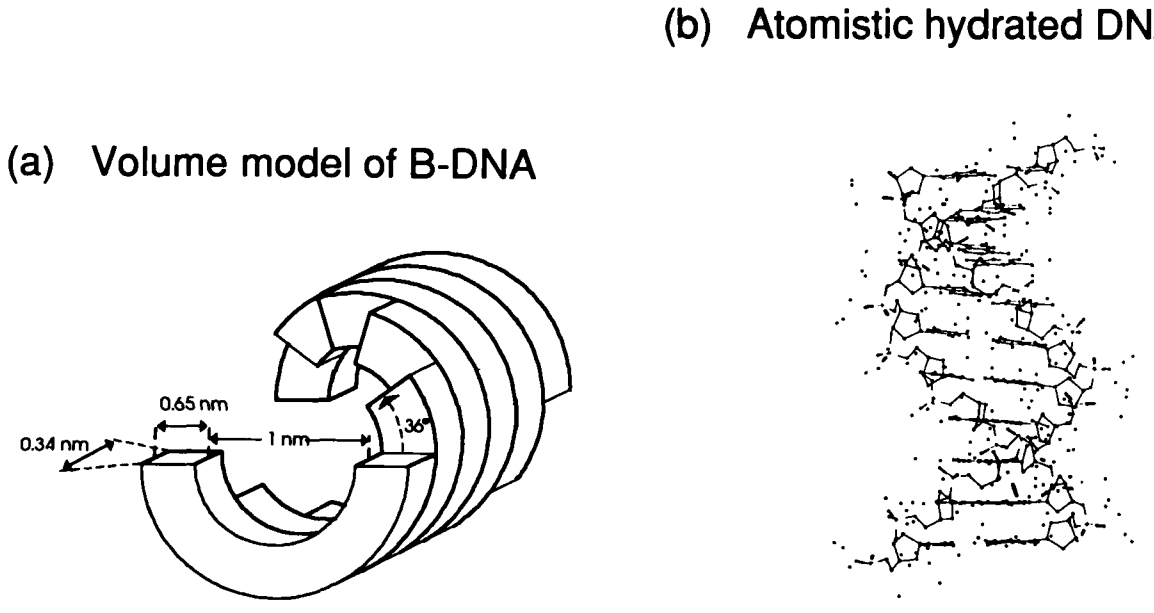

Fig. 2. Model of B-DNA. The volume model of B-DNA shows the volume of sugar-phosphate and the bases occupied by one nucleotide pair. The model implicitly contains the first hydration shell of the DNA within the volume of the sugar-phosphate and the bases. The atomistic model of the B-DNA is a decamer with the sequence CGCGAATTCG including the water molecules in the first hydration shell within 3.5 A of the polar atom.

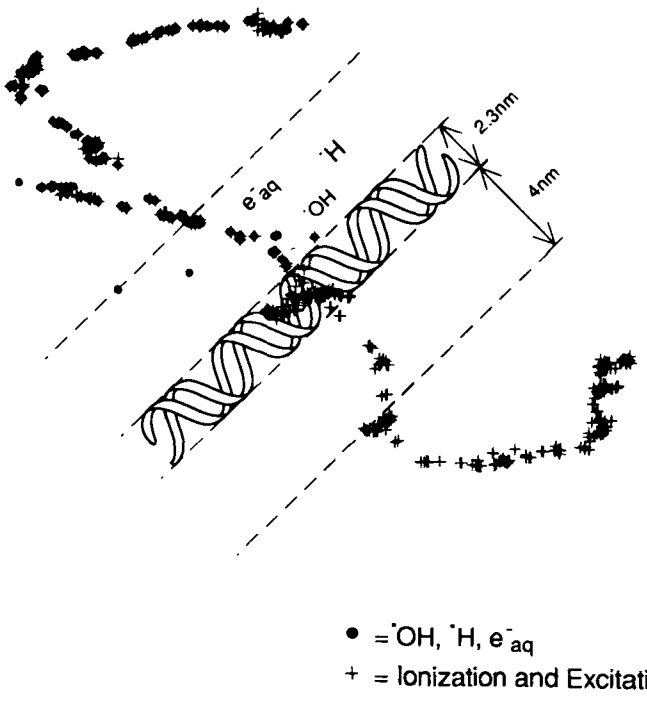

Fig. 3. Diagram illustrating the conceptual method of scoring DNA strand breaks induced by decay of iodine. The inner cylinder shows the double helical B-DNA with 2.3 nm diameter. The figure shows the tracks of all electrons released in 1 decay of the iodine which in this case contains 22 elctrons of various energies. The shaded area is the cylindrical shell around the DNA with a variable radius. The shell represent the bulk water around the DNA. The first hydration shell which is a structured bound water is shown in Figure 2b. The radius of cylindrical shell mimics the experimental condition of DNA environment. Interaction of electrons released in the decay of ^{125}I cause direct damage in the DNA modecule and generates radical species in the hydration shell around DNA. The reactive species ·OH, ·H, e^-_{aq} diffuse and could induce DNA damage. The probability of a reactive species reaching DNA is dependent on the DNA envirnoment. In a highly scavenging environment the radius of the cylindrical shell is very small—in limit reaching the condition of dry DNA. In a very dilute solution the radius of the cylindrical shell is very large being limited by the lifetime of the reactive species.

ing an ssb is not very precise in the sense that other values close to this were also in reasonable agreement with the experimental results (e.g., see ref. 8).

The agreement on the results of the Monte Carlo calculations with the experimental data provides some confidence in the Monte Carlo results. By analyzing the energy depositions in both of the strands and assuming that dsb was produced by ssbs separated by less than 10 base pairs, the yield of dsb per decay was calculated to be 0.9. In mammalian cells, an additional 0.2 breaks per decay would be produced by dose delivered to the cell nucleus by the longer ranged electrons. The results then were consistent with experiments with incorporated ^{125}I, which yielded 1 dsb per decay (4).

Through the estimate of breaks produced by each decay, the very complex and variable damage to the DNA was apparent. Dsb is not caused simply by scisson of the DNA but by several (if not many) occurring in the two single strands close to the decay site (9).

While the described results produced are encouraging, the model is empirical and overty simple. For example the energy depositions include all mechanisms—ionisation, excitation and sub-excitation whereas the latter two are unlikely to contribute greatly to DNA damage. Furthermore, the model does not provide for a mechanism to account for the effects of radical scavenging as observed by Rao et al. (9).

An alternative mechanism for DNA damage was discussed as early as in 1980 by Turner et al. (10) who considered the chemistry of the species initially formed in water in electron track, (·OH, e^-_{aq}, ·H), with particular attention to the production, diffusion and reactions of ·OH radicals).

Material and Methods

Recently, Nikjoo et al. (11) have developed a treatment to include the production, diffusion of chemical species and ·OH radical attack on DNA into the earlier model (12, 13) to produce a considerably more realistic treatment. This approach was used to analyze the results of a newly available high resolution repeat of the original Martin and Haseltine experiment (Kandaiya et al. this conference) which include the influence of scavenging DMSO. Calculations of single strand breaks use the Charlton et al. (14) Auger electron spectrum with the tracks of electrons and radical species, generated by the code CPA100 (15, 16) superimposed on an atomistic model of decamer B-DNA

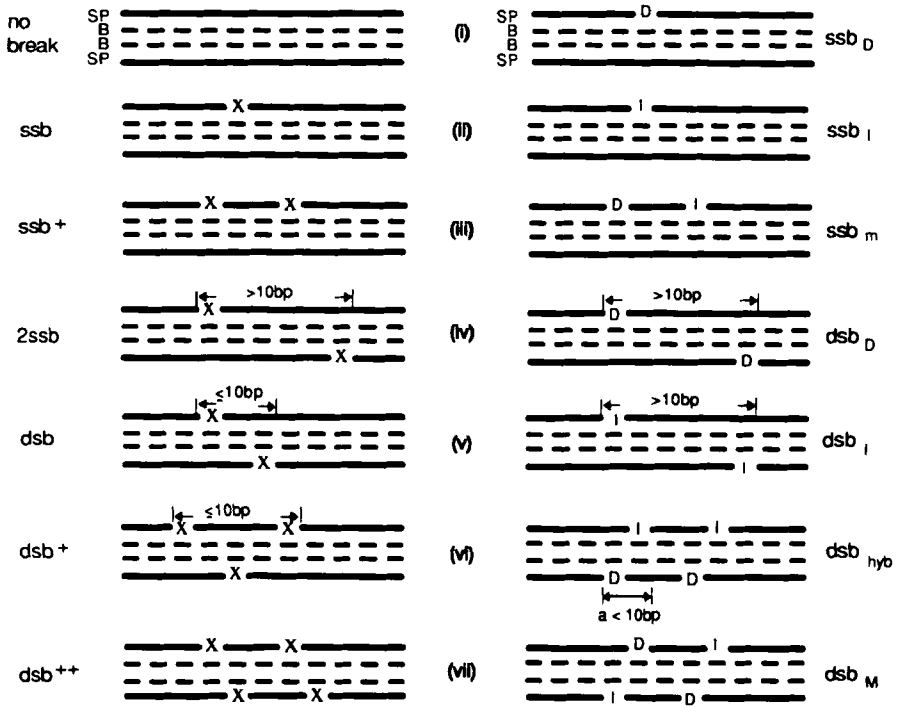

Fig. 4. Model of DNA damage. Various possible types of damage in the sugar-phosphate of the DNA induced by direct energy deposition or by the diffusing hydroxyl radicals. Only one type of damage assigned to DNA segment. On the left shown DNA damage indicated by an 'X'. Combination of one, two, three or greater than three single strand breaks on the same strand or on opposite strands have been assigned as 'ssb', 'ssb$^+$', '2ssb', 'dsb', 'dsb$^+$', and 'dsb^{++}'. The models on the right explicitly show the origin of the strand break 'X' whether arising from a direct energy deposition 'D', or from the activation of an 'OH radical.

(17) (Fig. 2b). The calculations were carried out for direct energy deposition events and for the hydroxyl radicals generated and diffusing in water of hydration around DNA.

General outlines

^{125}I decays first by electron capture (EC) to a metastable state of ^{125m}Te and then by internal conversion (IC) to ^{125}Te (14, 18, 19). The number of electrons in the cascade and their energies vary considerably depending on the initial inner shell vacancy and decay path. The starting point of these calculations is the simulation of electrons cascades released in the decay of iodine in IUdR incorporated in DNA molecule. The iodine spectrum used in this calculation is based on 10^4 individual decays.

The conceptual framework of the calculation is shown in Fig. 3. The method takes into account the interaction of the electron track in the DNA molecule from energy deposition events such as ionization and excitations due to direct effects ('short-range action') and contributions to the damage by hydroxyl radicals attacking the DNA ('long-term action').

The code CPA100 (20) follows the full slowing-down process of the electron to subexcitation and thermalization energies and the generation of radical species and molecular products (such as $^{\cdot}$H, $^{\cdot}$OH, e^-_{aq}, $^{\cdot}H^+$, $^{\cdot}OH^-$, H_2, H_2O_2, HO_2). In this physico-chemical stage (10^{-15}s – 10^{-12}s) the excited and ionized water molecules undergo several reactions leading to the formation of free radicals. Subexcitation electrons, i.e. electrons with kinetic energies less than 7.4 eV may recombine according to Onsager-Debye theory or lose energy by successive scattering until thermalization and formation of hydrated electrons. The diffusion and reaction rate constants and interaction distances for all

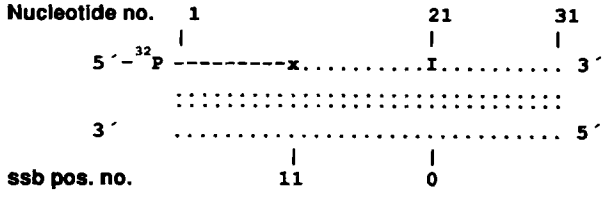

Fig. 5. A simplified representation of the oligonucleotide used in the experiment by Kandaiya et al. (this volume). The diagram shows the position of the iodine atom in nucleotide 21 and the end label of ^{32}P in the plasmid sequence. Only those fragments to the left of the iodine are detected in the upper strand.

radicals are those used in our previous calculations (11, 16).

Only those radicals generated in the cylindrical water shell surrounding the DNA were diffused and reacted from 10^{-12} s to 10^{-8} s using Smoluchowski's rule. In this calculation it is assumed that the DNA strand breakage is entirely due to damage in the sugar-phosphate skeleton and that base modifications do not lead to strand break (21). The radius of the cylindrical water shell around the DNA is reduced to mimic the high scavenging condition or increased to lower the scavengeable concentration of the medium surrounding the DNA as shown in Fig. 3. In addition the scavengeable conditions is controlled by the diffusion time and the activation probability of the 'OH radicals.

Model of DNA and DNA damage

Fig. 2 shows the two models of canonical B-DNA decamers we have used in previous and present calculations. The volume model is the one originally used by Charlton (8) while the atomistic model includes the hydration shell which enables us to follow the ensuing chemistry in more detail (17). A preliminary test was first made to ascertain to what extent the two models differ in the present calculations. From our test we concluded that without consideration of the entire mechanics of strand break induction (22–24) the two models of the DNA produce similar results, and thus shows that the simpler volume model used up to date is applicable.

The model of damage, Fig. 4, considers induction of strand breaks and clusters of them by direct energy deposi-

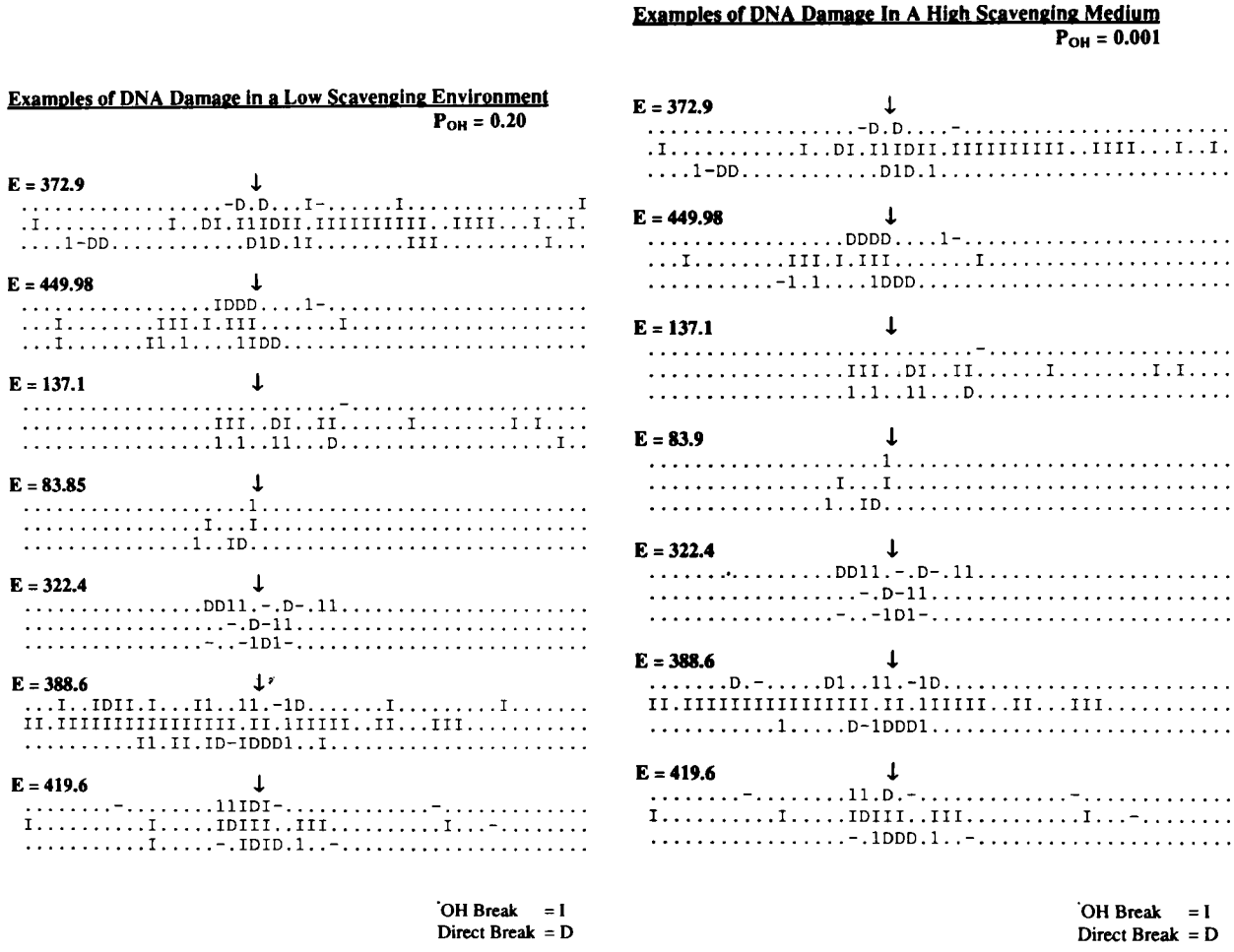

Fig. 6. Two sets of individual examples of each iodine decay in the DNA. In all cases the radius of the hydration shell was set at 4 nm and radicals were diffused from the initial time of 10^{-12} s to 10^{-8} s. a) Examples of breaks induced by electrons and radicals in a very high scavenging medium – 'OH activation probability was set at 0.001, thereby mimicking the case of direct effect when all radicals have scavenged away before reaching DNA. b) In this case examples of the same decay as in a) are shown with 'OH activation probability of 0.20. The total energy E deposited in the DNA is shown above each DNA segment. The energy is the energy of events—ionizations and excitations deposited in the nucleotide for 'direct breaks'. Position of the iodine at nucleotide 21 is indicated by an arrow. 'D' and 'I' indicate induction of a ssb by direct energy deposition or by 'OH radicals respectively. A 'l' represents energy deposition less than 17.5 eV and a '–' less than 10 eV. We assume 80% of 'OH radicals react with the basis and 20% with sugar-phosphate (11).

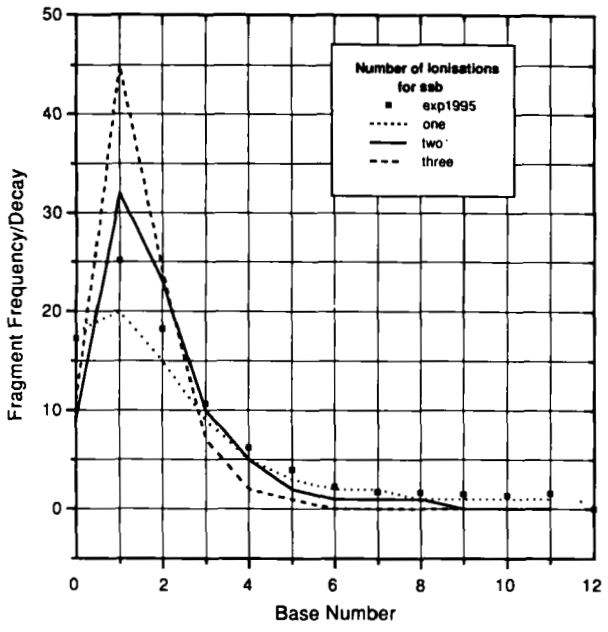

Fig. 7. Distribution of the farthest distances to the single strand break from the site of the iodine. In this calculation it was assumed that ionizations, rather than the energy deposition, was the event leading to a strand break.

tion in the sugar-phosphate skeleton and by diffusing hydroxyl radicals. Fig. 4 shows possible clustering forms of single-strand breaks on one or both strands; 'no break' signifies that the energy deposition events and radical attack in the sugar phosphate did not lead to strand breakage, 'SSB' indicates a single-strand break from a direct energy deposition event (ssb_D) or from an activating 'OH radical (ssb_I). Combination of 2 single-strand breaks on opposite strands can lead to a '2SSB' or a double-strand break 'DSB', depending on the separation distance 'a' between the two breaks. Fig. 4(vi–vii) shows higher orders of clustering of 'ssb's forming complex double strand breaks and deletions. Again, each strand break could be a 'ssb_I' or a 'ssb_D' giving a 'dsb_{hyb}'–when a single-strand break converted into a double-strand break by an 'OH radical. Each 'D' or 'I' represent a strand break or a base damage induced by direct energy deposition by a single event including ionizations and excitations or by an 'OH radical.

The lower threshold for strand breakage due to direct energy deposition was set at 17.5 eV and mimicking the experimental condition an activation probability p was assigned to 'OH radicals inducing damage leading to strand break.

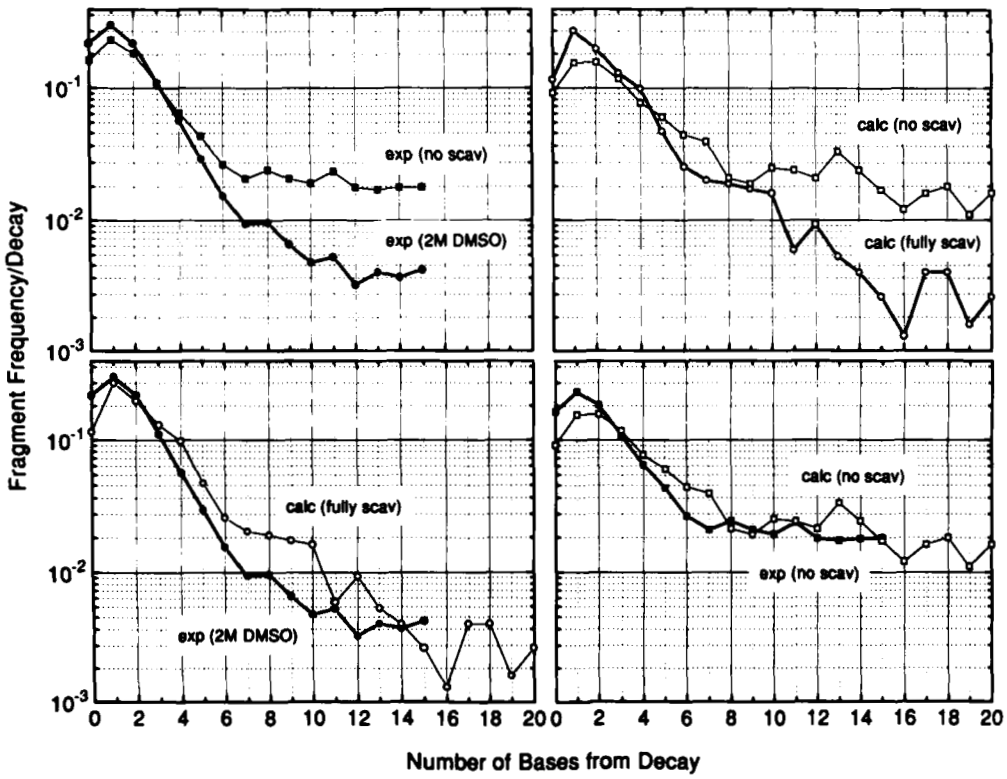

Fig. 8. The frequency of the distances of the farthest strand breaks produced in the chain containing the iodine. The data has been compared with experiments of Kandaiya et al. (this volume). Top-left panel shows data for experiments with 2M DMSO and no-scavenger added. The top-right panel presents corresponding calculated data. The two lower panels show the comparison between the experiments and the calculated data for the experiments with 2M DMSO added and no-scavenger added. Top-left panel show the experimental data. The unscavenged data is shown by solid squares, upper curve (lighter line), and the lower curve for 2M DMSO, solid circles (heavy line). The top-right panel shows the corresponding curve for the calculations and the two lower panels show the comparison with the experiments. Only 1000 decays were scored for this calculation.

Results and Discussion

Fig. 5 gives a pictorial description of the Kandaiya et al. experiment. A short fragment of a 31-mer double-stranded oligodeoxynucleotide containing ^{125}I at the position 21 was end-labelled with ^{32}P in the strand containing the iodine-labelled base. The position of the farthest single-strand breakage produced from a decay of ^{125}I is marked with 'X' at nucleotide number 11 giving a fragment length of 9 nucleotides in length. We have calculated the fragment lengths of the DNA in the same manner as in the experiment using a canonical B-DNA sequence.

The experiment measured the length of fragments produced by single-strand breaks. In the calculation we need to assume pathways leading to induction of a single-strand break. A single-strand break could be a consequence of energy deposition event leading to ionization of the target molecule or attack by 'OH radicals. We have included three of the above mechanisms that could induce single-strand breaks in the DNA: Fig. 6 shows examples of strand breaks produced in DNA by iodine decay in two different environments. The arrows show the position of the incorporated iodine.

Fig. 7 shows an alternative way of estimating a relationship between the physical event and a biological endpoint by using ionizations in the sugar phosphate volume of Fig. 2a. The calculated data have been compared with the experimental data for the short-range damage (direct effect). The data show the frequency of producing a fragment due to a single-strand break due to one, two or three ionizations, in the sugar-phosphate. The solid curve, two ionizations, gives a reasonable agreement with the experiment. Fig. 8, in 4 panels, shows the results of different experimental conditions, including comparison of DNA breaks obtained with and without the radical scavenger dimethyl sulphoxide (DMSO).

We have thus re-examined the relationship between energy deposition due to the decay of ^{125}I and the appearances of strand breaks on the basis of a new experimental data and a more sophisticated method of calculation, taking into account the damage induced by direct energy deposition and the radical species generated in vicinity of the target atoms. The original relationship between the energy deposition 17.5 eV and induction of a single-strand break was confirmed. In these calculations we assumed the transport of charged particles in DNA to be similar to that of liquid water. To what extent the phase effect and boundary conditions in DNA affects the results of strand breaks and how realistic is the pathway adopted for induction of strand breaks and what is the possible role of bases in mediating damage in DNA? To answer such questions and others, we need to consider the dynamics of the DNA molecule and its environment in relation to the transport of charged particles which necessitates a more clear understanding of the molecular nature of the DNA damage.

ACKNOWLEDGEMENTS

The authors wish to thank Philippa Middlehurst and Kevin Glover for helping with the preparation of this manuscript.

REFERENCES

1. Krish RE, Krasin F, Sauri CJ. DNA breakage, repair and lethality accompanying ^{125}I decay in micro-organisms. Curr Top Radiat Res Q 1977; 12: 355–68.
2. Martin RF, Haseltine WA. Range of radiochemical damage to DNA with decay of iodine-125. Science 1981; 213: 896–8.
3. Terrissol M, Patau JP, Eudaldo T. Application a la microdosimetric et a la radiobiologie de la simulation du transport des electron de basse energie dans l'eau a l'etat liquide. In: Booz J, Ebert HG, Smith BGR, eds. Proceedings of the 6th Symposium on Microdosimetry. London: Harwood Academic, 1978: 169–82.
4. Paretzke HG. Advances in energy deposition theory. In: Thomas RH, Perez-Mendez V, eds. Advances in Radiation Protection and Dosimetry in Medicine. New York: Plenum, 1980: 51–73.
5. Charlton DE. The range of high LET effects from ^{125}I decays. Radiat Res 1986; 107: 163–71.
6. Charlton D. DNA damage by Auger emitters, London: Taylor and Francis, 1988.
7. Charlton DE, Humm JL. A method of calculating initial DNA strand breakage following the decay of incorporated ^{125}I. Int J Radiat Biol 1988; 53: 353–65.
8. Pomplun E, Roch M, Terrissol M. Simulation of strand break induction by DNA incorporated ^{125}I. In: Howell RW, Narra VR, Sastry KSR, Rao DV, eds. Biophysical aspects of Auger processes: AAPMS symposium series No. 8. 1992: 137–52.
9. Rao DV, Ventateswara RN, Howell RW, Sastry KSR. Biological consequence of nuclear versus cytoplasmic decays of ^{125}I: Cysteamine as a radioprotector against Auger cascades in vivo. Radiat Res 1990; 124: 188–93.
10. Turner JE, Hamm RN, Wright HA, Richie RH. Early events in irradiated water, 7th Microdosimetry 1978; 507–20.
11. Nikjoo H, O'Neill P, Terrissol M, Goodhead DT. Modelling of radiation-induced DNA damage: the early physical and chemical events. Int J Radiat Biol 1994; 66: 453–7.
12. Charlton DE, Booz J. A Monte Carlo treatment of the decay of ^{125}I. Radiat Res 1981; 87: 10–23.
13. Terrissol M. Modelling of radiation-induced DNA damage: the early phsyical and chemical events. Int J Radiat Biol 1994; 66: 447–51.
14. Charlton DE, Nikjoo H, Humm JL. Calculation of initial yields of single- and double-strand breaks in cell nuclei from electrons, protons and alpha particles. Int J Radiat Biol 1989; 56: 1–19.
15. Nikjoo H, Charlton DE, Goodhead DT. Monte Carlo track structure studies of energy deposition and calculation of initial DSB and RBE. Adv Space Res 1995; 14: 161–80.
16. Terrissol M, Beaudre A. Simulation of space and time evolution of radiolytic species induced by in water. Radiat Prot Dosim 1990; 31: 171–5.
17. Umrania Y, Nikjoo H, Goodfellow J. A knowledge-based model of DNA hydration. Int J Radiat Biol 1995; 66: 453–7.
18. Feinendegen LE. Radiation environmental Biophysics 1975; 12: 85.
19. Hofer KG. Radiation biology and potential of theraputic application of radionuclides. Bull Cancer (Paris) 1980; 67: 343–53.

20. Nikjoo H, Terrissol M, Hamm RN, et al. Comparison of energy deposition in small cylindrical volumes by electrons generated by Monte Carlo track structure codes for gaseous and liquid water. Radiat Prot Dosim 1994; 52: 161–5.
21. Ward JF, Milligan JR, Jones GDD, Fahey RC. Multiply damaged sites. In: Fuciarelli AF, Zimbrick JD, eds. Radiation damage in DNA: Structure/function relationships at early times. Battelle Press, 1995.
22. Zaider M, Bardash M, Fung A. Molecular damage induced directly and indirectly by ionizing radiation in DNA. Int J Radiat Biol 1994; 66: 453–7.
23. von Sonntag C. The chemical basis of radiation biology. London: Taylor and Francis, 1987: 275–9.